Short Communication

CONTRAST MEDIA & MOLECULAR IMAGING

Received: 23 April 2012, Revised: 21 August 2012, Accepted: 29 August 2012, Published online in Wiley Online Library

(wileyonlinelibrary.com) DOI: 10.1002/cmmi.1509

Quantitative imaging of the tissue contrast agent $[Gd(DTPA)]^{2-}$ in articular cartilage by laser ablation inductively coupled plasma mass spectrometry

Alessandra Sussulini[a†‡], Edzard Wiener[b‡], Tim Marnitz[b], Bei Wu[a], Berit Müller[c], Bernd Hamm[b] and J. Sabine Becker[a*]

Laser ablation inductively coupled plasma mass spectrometry (LA-ICP-MS) is an emerging analytical technique in the generation of quantitative images of MR contrast agent distribution in thin tissue sections of articular cartilage. An analytical protocol is described that includes sample preparation by cryo-cutting of tissue sections, mass spectrometric measurements by LA-ICP-MS and quantification of gadolinium images by one-point calibration, standard addition method (employing matrix-matched laboratory standards) and isotope dilution analysis using highly enriched stable Gd-155 isotope (abundance 92 vs 14.8% in the $[Gd(DTPA)]^{2-}$ contrast agent). The tissue contrast agent concentrations of $[Gd(DTPA)]^{2-}$ in cartilage measured in this work are in agreement with findings obtained by magnetic resonance imaging and other analytical methodologies. The LA-ICP-MS imaging data also confirm the observation that the spatial distribution of $[Gd(DTPA)]^{2-}$ in the near-equilibrium state is highly inhomogeneous across cartilage thickness with the highest concentration measured in superficial cartilage and a strong decrease toward the subchondral bone. In the present work, it is shown for the first time that LA-ICP-MS can be applied to validate the results from quantitative gadolinium-enhanced MRI technique of articular cartilage. Copyright © 2012 John Wiley & Sons, Ltd.

Keywords: MRI contrast agents; gadolinium; articular cartilage; imaging; LA-ICP-MS; quantification

1. INTRODUCTION

Delayed gadolinium-enhanced MRI of cartilage is widely used to quantify proteoglycan (PG) loss in early cartilage degradation. Prior work has shown that the distribution of the negatively charged gadopentetate dimeglumine molecules $[Gd(DTPA)]^{2-}$ (molecular weight, 938 g mol^{-1}; molecular net charge of the gadopentetate chelate, –2) in the near-equilibrium state is a good measure of the PG distribution in cartilage (1–6). The precision of the quantification of the PG content depends on an adequate measurement of $[Gd(DTPA)]^{2-}$ concentration in cartilage tissue $[Gd(DTPA)]^{2-}$. According to the equation:

$$\Delta R_1 = \left(R_{1,\text{after}} - R_{1,\text{before}}\right) = [\text{Gd(DTPA)}]^{2-} . r_{1,\text{Gd}},$$

measurements of the longitudinal MR relaxation rate R_1 in cartilage before ($R_{1,\text{before}}$) and after ($R_{1,\text{after}}$) Gd administration can be used to calculate the tissue contrast agent concentration. The relaxivity of $[Gd(DTPA)]^{2-}$ $r_{1,\text{Gd}}$ in healthy and diseased cartilage is unknown and a constant *r*-value obtained from saline or solid milk solution is used (7–10). The *r*-value of $[Gd(DTPA)]^{2-}$ in articular cartilage is a critically important parameter in the quantification of tissue contrast agent concentration using MRI. Independent methods have to be established to verify these MR results. Furthermore, MRI cannot provide information regarding the inorganic elements' spatial distribution, which is related to the continuous breakdown and remodeling of the extracellular matrix in healthy and diseased cartilage. The macromolecular content in different cartilage layers is correlated with the elemental distribution and the function of several cartilage enzymes rely on the presence of metallic cofactors (11,12). The local concentration of divalent cations is therefore of considerable interest in articular cartilage pathophysiology.

The current feasibility study presents a novel application of laser ablation inductively coupled plasma mass spectrometry (LA-ICP-MS) imaging technique that can be used to quantify spatially resolved $[Gd(DTPA)]^{2-}$ concentrations in cartilage. This powerful and versatile analytical technique provides direct information about the spatial distribution of elements, present at

* *Correspondence to: Becker, J. Sabine, Central Division of Analytical Chemistry, Forschungszentrum Jülich, D-52425, Jülich, Germany. E-mail: s.becker@fz-juelich.de*

† *Current address: Pontifical Catholic University of Rio de Janeiro (PUC-Rio), Department of Chemistry, Rua Marquês de São Vicente 225, Gávea, 22453-900, Rio de Janeiro, RJ, Brazil*

‡ *The first two authors contributed equally.*

a *A. Sussulini, B. Wu, J. Sabine Becker*
Central Division of Analytical Chemistry, Forschungszentrum Jülich, D-52425 Jülich, Germany

b *E. Wiener, T. Marnitz, B. Hamm*
Charité – Universitätsmedizin Berlin, Department of Radiology, Charitéplatz 1, D-10117 Berlin, Germany

c *B. Müller*
Charité – Universitätsmedizin Berlin, Department of Pathology, Charitéplatz 1, D-10117 Berlin, Germany

very low concentrations ($\mu g\,g^{-1}$ to $ng\,g^{-1}$ range) in biological tissue sections. LA-ICP-MS has been used for quantitative mass spectrometric imaging (MSI) of elements in different biological (e.g. study of neurodegenerative diseases in brain samples) and environmental (e.g. accumulation of essential elements in leaves) applications, as reviewed in a recently published textbook and many reviews (13–15). The main advantages of this technique are: low detection limits for most elements; minimal matrix effects; specific response for different elements (metals, metalloids or nonmetals); and information about isotope ratios that can be applied for exact and precise quantification using isotope dilution analysis (13).

Kamaly *et al*. (16) used LA-ICP-MS for post-mortem imaging of gadolinium spatial distribution in a mouse tumor model after administration of PEGylated gadolinium liposomal nanoparticles. The presence of gadolinium within tumor tissue was confirmed by LA-ICP-MS and when correlated to histology was found to be prevalent in regions of higher vascularity. The presence of gadolinium in the kidneys was also confirmed. In another work, Hsieh *et al*. (17) used LA-ICP-MS to map the spatial distribution of gadolinium-doped iron oxide nanoparticles in one tumor slice that had been subjected to magnetic fluid hyperthermia. The mapping results revealed the high resolution of the elemental analysis, with the distribution of gadolinium atoms highly correlated with that of the iron atoms, presumably reflecting the distribution of the injected magnetic fluid. Although these are the pioneer works involving the application of LA-ICP-MS to detect gadolinium in biological samples, quantification was not performed. The first work showing quantitative LA-ICP-MS images of gadolinium in biological tissue was performed by Pugh *et al*. (18). The authors determined gadolinium and zinc concentrations in Gd–DOTA–colchicinic acid-dosed tumors from mice using a calibration strategy based on matrix-matched standards.

Table 1. Obtained gadolinium concentrations in cartilage (for superficial and deep regions) by the different analytical strategies employed

	Determined Gd concentrations ($mmol\,l^{-1}$)	
Method	Superficial region	Deep region
Standard addition	1.06 ± 0.03	0.64 ± 0.04
One-point calibration	1.12 ± 0.07	0.67 ± 0.06
Isotope dilution analysis	1.1 ± 0.2	0.7 ± 0.1

To the best of our knowledge, this is the first study using LA-ICP-MS for quantitative imaging of $[Gd(DTPA)]^{2-}$ and qualitative imaging of other metals and nonmetals in articular cartilage.

2. RESULTS AND DISCUSSION

Articular cartilage is an inhomogeneous tissue with a zonal anatomy and a nonuniform distribution of macromolecular content with increasing PG concentration and decreasing collagen concentration from superficial to deeper layers (19–23). This heterogeneity of articular cartilage makes the quantification of tissue contrast agent concentration by MRI challenging because the spatially distributed gadolinium relaxivity in cartilage is unknown. A few MR studies that have considered this topic have used a constant gadolinium relaxivity value $r_{1,Gd} \approx 7\,mmol\,l^{-1}\,s^{-1}$ in hyaline cartilage that came from measurements in 30% solid milk solution at 1.5 T (8). This approximation is based on the assumption that the gadolinium relaxivity in biological tissue should be a function of its solid composition content (8).

Previous publications have measured a relaxation rate difference in superficial cartilage layers after $[Gd(DTPA)]^{2-}$ administration in the near-equilibrium state of $\Delta R_1 \approx 8\,s^{-1}$ at 1.5 T (24–26). Combining these data with the relaxivity $r_{1,Gd} \approx 7\,mmol\,l^{-1}\,s^{-1}$ of $[Gd(DTPA)]^{2-}$ for a macromolecular content of about 30% (8), the $[Gd(DTPA)]^{2-}$ concentration in superficial cartilage can be calculated as $[Gd(DTPA)]^{2-} = \Delta R_1 / r_{1,Gd} \approx 1.1\,mmol\,l^{-1}$. This result is in excellent agreement with our measurements performed by LA-ICP-MS, as described in Tables 1, and using different analytical strategies for quantification: one-point calibration, standard addition method (figures of merit described in Table 2) and isotope dilution analysis.

The obtained data also confirm the observation that the spatial distribution of $[Gd(DTPA)]^{2-}$ in the near-equilibrium state is highly inhomogeneous across cartilage thickness with the highest concentration measured in superficial cartilage layers and a strong decrease toward the subchondral bone (26,27), which is shown in Figs 1 and 2 for all the gadolinium isotopes measured by LA-ICP-MS.

Figure 1 shows LA-ICP-MS images of the detected metals (sodium, magnesium, potassium, calcium, titanium and zinc) and nonmetals (carbon, phosphorus, sulfur and chlorine) in articular cartilage tissue. Sodium, chlorine and potassium, were detected with a higher accumulation in superficial cartilage layers compared with deep cartilage layers, whereas the concentration gradients of

Table 2. Figures of merit from standard addition method

Gd isotope	Calibration curve	Correlation coefficient (R^2)	Limit of detection ($\mu mol\,l^{-1}$)[a]	Limit of quantification ($\mu mol\,l^{-1}$)[b]
^{152}Gd	$y = 1753.5x - 291.95$	0.9938	7.03	23.4
^{154}Gd	$y = 19801x - 4802.5$	0.9931	0.68	2.27
^{155}Gd	$y = 137626x - 34177$	0.9931	0.02	0.05
^{156}Gd	$y = 195595x - 50194$	0.9925	0.06	0.20
^{157}Gd	$y = 150540x - 37908$	0.9932	0.10	0.32
^{158}Gd	$y = 247550x - 64837$	0.9927	0.01	0.04
^{160}Gd	$y = 223433x - 56625$	0.9929	0.01	0.03

[a]Calculated as 3 times the standard deviation of the blank divided by the slope from the calibration curve.
[b]Calculated as 10 times the standard deviation of the blank divided by the slope from the calibration curve.

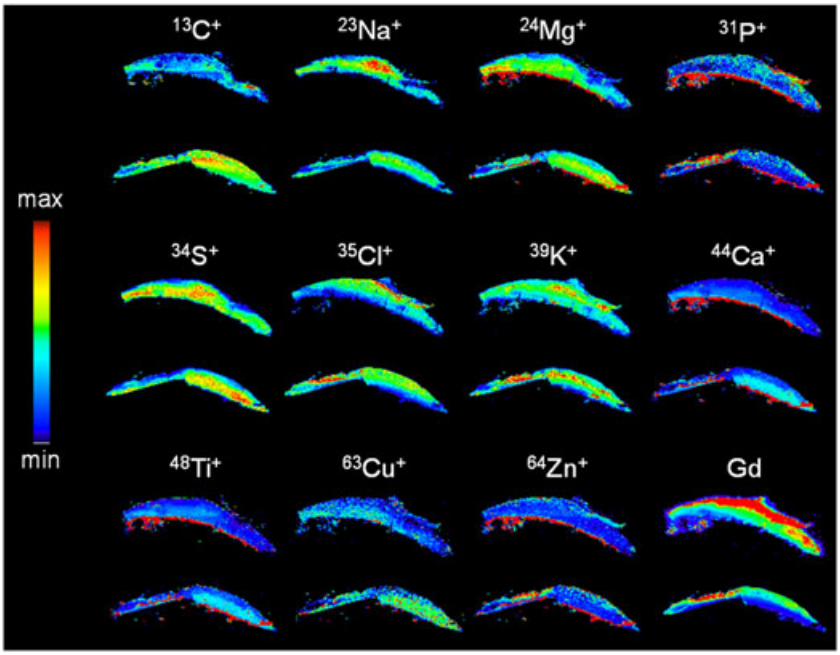

Figure 1. Representative LA-ICP-MS maps of gadolinium, carbon, sodium, magnesium, phosphorus, sulfur, chlorine, potassium, calcium, titanium, copper and zinc isotope as detected in articular cartilage for two samples.

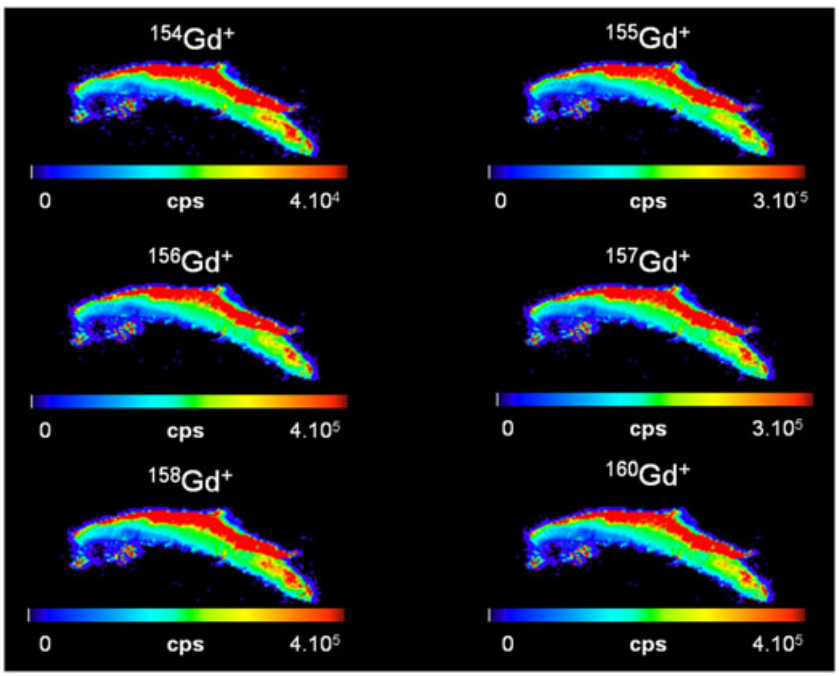

Figure 2. LA-ICP-MS imaging of gadolinium isotopes distribution in articular cartilage treated with $[Gd(DTPA)]^{2-}$ contrast agent.

magnesium, phosphorus, calcium, titanium and zinc increased from cartilage surface toward the calcified region (Tidemark) and subchondral bone. Similar findings have been reported in previous studies using synchrotron radiation-induced X-ray emission (28) and micro-proton induced X-ray emission (11). Elemental imaging of articular cartilage by LA-ICP-MS, especially that of sulfur (indicator for proteoglycans) (29), carbon (indicator for collagen) (30) or co-factor trace element such as zinc, calcium and phosphorus (indicators for cartilage degradative enzymes) (11) compared with MR findings will considerably improve our understanding of articular cartilage pathophysiology.

Figure 2 shows the gadolinium isotopes measured for a cartilage sample treated with 2.0 mmol l^{-1} $[Gd(DTPA)]^{2-}$ contrast agent. The distribution of gadolinium for all measured isotopes in articular

cartilage is the same. The observed gadolinium distribution by LA-ICP-MS is in accordance with the MRI findings (see Fig. 3) and can be explained by the different macromolecular content of superficial and deep cartilage layers.

Performing elemental imaging by LA-ICP-MS has the advantages of eliminating labor-intensive sample preparation and reducing spectral interference and contamination because no steps of digestion and dilution are required, increasing the analyte throughput, as well as allowing *in situ* qualitative/quantitative determination of the inorganic species present in thin tissue sections (31). Detection by LA-ICP-MS is fast and fairly robust, as no further reaction or derivatization step is involved (as with some separation techniques), and the signal is, theoretically, directly proportional to the amount of the element present in the tissue. This technique is applied for microlocal analysis of solid samples, with spatial resolution usually in the 110–4 μm range (depending on the laser ablation system used), providing an accurate sampling of small volumes or amounts of biological, medical or environmental samples (13,15,31).

An appropriate quantification of the $[Gd(DTPA)]^{2-}$ concentration in cartilage tissue is critically important in the calculation of the PG content by MRI. We have shown for the first time that LA-ICP-MS can be used to explain results from quantitative gadolinium enhanced MRI technique in articular cartilage.

3. CONCLUSION

The present work shows that LA-ICP-MS can be applied to validate the results from gadolinium enhanced MRI technique. The measured tissue contrast agent concentrations $[Gd(DTPA)]^{2-}$ in cartilage are in good agreement with the results previously reported by MRI, and the analytical methodologies used for quantification, one-point calibration, standard addition method and isotope dilution analysis provided similar results (1.12 ± 0.07, 1.06 ± 0.03 and 1.1 ± 0.2 mmol l^{-1}, respectively). The LA-ICP-MS imaging data also corroborate the observation that the spatial distribution of $[Gd(DTPA)]^{2-}$ in the near-equilibrium state is highly inhomogeneous across cartilage thickness with the highest concentration measured in superficial cartilage and a strong decrease toward the subchondral bone.

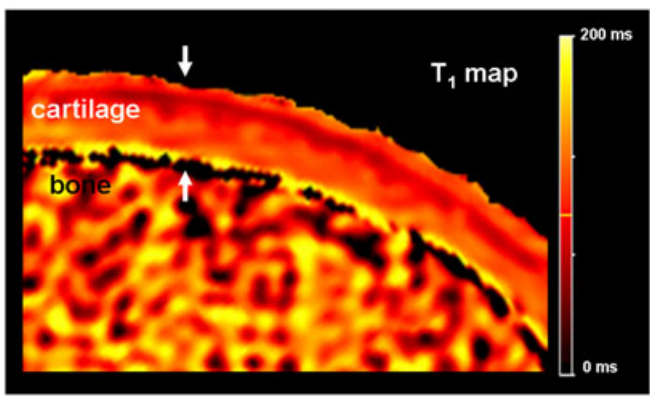

Figure 3. Axial MR T_1 map shows T_1 distribution after immersion in gadolinium solution (24 h). T_1 values are inversely correlated to the gadolinium concentration in articular cartilage.

4. EXPERIMENTAL

4.1. Cartilage sample preparation

Twelve bovine patellae ($n = 12$) were obtained successively from freshly slaughtered animals. Three specimens ($n = 3$) were placed in 250 ml of 2.0 mmol l^{-1} gadopentetate dimeglumine $[Gd(DTPA)]^{2-}$ contrast solution (Magnevist, Schering, Germany), typically used for direct MR arthrography. Three specimens ($n = 3$) were placed in saline for control. After 24 h of immersion, patellae specimens were imaged and sectioned with a band saw perpendicular to the cartilage surface. The cartilage samples were cut in thin sections (30 μm thick) with a cryomicrotome. The sections were placed on microscopic slides for LA-ICP-MS imaging.

4.2. MRI – T_1 mapping

All imaging was performed with a 1.5 T system (Magnetom, Avanto; Siemens Healthcare, Erlangen, Germany) using an eight-channel knee coil. For T_1 mapping of the entire patellae, a dual flip-angle 3D gradient echo sequence was used in the axial plane. The sequence parameters were: repetition time, 15.0 ms; echo time, 2.06 ms; flip angle, 5 and 26°; effective section thickness, 2.5 mm; number of excitations, two; field of view, 10 × 10 cm; and matrix, 256 × 256 (pixel spacing 0.39 × 0.39 mm). The acquisition time was 4.52 min. For the calculation of parametric maps of T_1 the automated tool syngo Mapit (Siemens Healthcare, Erlangen, Germany) was used. The T_1 values obtained with the dual flip-angle 3D gradient echo sequence are in good agreement with previous measurements (26).

4.3. LA-ICP-MS measurements and data treatment

A laser ablation system (New Wave UP213, Fremont, CA, USA) hyphenated with a quadrupole-based ICP mass spectrometer (XSeries II, Thermo Fischer Scientific, Bremen, Germany) was used for elemental imaging analyses and quantification of gadolinium in cartilage samples. For imaging experiments, a defined sample area was ablated line by line with a focused Nd–YAG laser beam. The ablated material was transported by the carrier gas into the ICP. Then, the formed ions were extracted and analyzed in the quadrupole mass spectrometer according to their mass-to

Table 3. Optimized experimental parameters used for LA-ICP-MS imaging of articular cartilage samples

ICP mass spectrometer	ICP-QMS, Thermo XSeries II
RF power	1500 W
Carrier gas flow rate	1.0 l min^{-1}
Mass resolution ($m/\Delta m$)	300
Laser ablation system	New Wave UP 213
Wavelength of Nd–YAG laser	213 nm
Laser pulse duration	20 ns
Repetition frequency	20 Hz
Laser energy per pulse	7 μJ
Laser fluence	0.25 J cm^{-2}
Scan speed	60 μm s^{-1}
Dwell time	30 ms
Laser spot size	60 μm
Distance between lines	30 μm

charge ratio (*m/z*). Table 3 summarizes the optimized experimental parameters employed for LA-ICP-MS analyses. To validate the obtained results, at least two isotopes, if available (e.g. $^{63}Cu^{+}$ and $^{65}Cu^{+}$), were analyzed. For gadolinium, six isotopes were measured. Possible isobaric interferences of single-charged analyte ions with polyatomic or double-charged ions were studied systematically and minimized under the optimized experimental conditions. The carrier gas for laser ablated material was argon. Isobaric interferences of atomic ions of analyte and disturbing polyatomic ions of argon at the same nominal mass (such as $^{56}Fe^{+}$ and ArO^{+}) were considered carefully by subtraction of the – in general constant – background intensity. By measurement of isotope ratios of images and comparison with the IUPAC table values, possible isobaric interferences can be easily detected. Images of interference-free isotopes were selected for evaluation.

For the quantification of LA-ICP-MS imaging data, matrix-matched laboratory standards were prepared by adding gadolinium solutions at different concentrations in powder cartilage samples. Cartilage powder was prepared using a high speed surgical rotary cutter that was directed over the cartilage surface of untreated patellae ($n = 6$). The cartilage powder was collected and divided in four portions of 530 mg each. The samples were doped with different concentration of gadolinium solutions, homogenized and dried in a dehydrator until the initial weight of 530 mg was achieved again. Cartilage powder samples with four different concentrations of $[Gd(DTPA)]^{2-}$ were prepared (75, 150, 250 and 500 $\mu g\,g^{-1}$). Another cartilage powder sample was doped with 2 $mmol\,l^{-1}$ gadolinium solution and was used for quantification by one-point calibration.

For isotope dilution analysis experiments, spike solutions of highly enriched stable Gd-155 isotope (abundance 92 vs 14.8% in the $[Gd(DTPA)]^{2-}$ contrast agent, according to the IUPAC table value of isotopic abundance in nature) were directly added to the powder cartilage samples previously immersed in 2.0 $mmol\,l^{-1}$ $[Gd(DTPA)]^{2-}$ solution. The mixtures were then homogenized, dried and pressed to pellets, as described elsewhere (32). These pellets were analyzed by LA-ICP-MS and the gadolinium concentration in the sample was calculated according to the isotope dilution equation:

$$c_{\text{sample}} = c_{\text{spike}} \cdot \frac{m_{\text{spike}}}{m_{\text{sample}}} \cdot \frac{M_{\text{sample}}}{M_{\text{spike}}} \cdot \frac{A^{b}_{\text{spike}}}{A^{a}_{\text{sample}}} \left(\frac{R_m - R_{\text{spike}}}{1 - R_m \cdot R_{\text{sample}}} \right)$$

where R_{sample} (calculated on the basis of IUPAC tabulated values) and R_{spike} (calculated from the certificate of the spike material) are the isotope ratios between isotopes *a* (reference) and *b* (the most abundant in the spike) in the sample and spike, respectively; m_{sample} and m_{spike} are the masses of sample and spike, respectively; M_{sample} and M_{spike} are the standard atomic masses of isotopes *a* and *b*; A^{a}_{sample} and A^{b}_{spike} are the percentages of isotopes *a* and *b* in the sample and in the spike, respectively; c_{spike} is the concentration of the element in the spike; and R_m is the ratio between isotopes *a* and *b*, obtained experimentally by LA-ICP-MS (13,32–36). Reverse isotope dilution equations were used to determine the gadolinium concentration in the spike (36).

Elemental LA-ICP-MS images were reconstructed from the continuous list of raw data points, present as text file containing a data column of every measured isotope, visualized and converted into 8 bit TIFF files using IMAGENA software (37).

Acknowledgments

A.S. would like to thank the Alexander von Humboldt Foundation (Bonn, Germany) for the postdoctoral fellowship. The last author (J.S.B.) would like to acknowledge Thermo Scientific (Bremen, Germany) and Deutsche Forschungsgemeinschaft (DFG grant number BE 2649/5-1) for instrumental support of the BrainMet laboratory.

REFERENCES

1. Bashir A, Gray ML, Burstein D. Gd-DTPA^{2-} as a measure of cartilage degradation. Magn Reson Med 1996; 36(5): 665–673.
2. Bashir A, Gray ML, Boutin RD, Burstein D. Glycosaminoglycan in articular cartilage: in vivo assessment with delayed Gd(DTPA)(2−)-enhanced MR imaging. Radiology 1997; 205(2): 551–558.
3. Trattnig S, Mlynarik V, Breitenseher M, Huber M, Zembsch A, Rand T, Imhof H. MRI visualization of proteoglycan depletion in articular cartilage via intravenous administration of Gd-DTPA. Magn Reson Imag 1999; 17(4): 577–583.
4. Nieminen MT, Rieppo J, Silvennoinen J, Toyras J, Hakumaki JM, Hyttinen MM, Helminen HJ, Jurvelin JS. Spatial assessment of articular cartilage proteoglycans with Gd-DTPA-enhanced T1 imaging. Magn Reson Med 2002; 48(4): 640–648.
5. Laurent D, Wasvary J, Rudin M, O'Byrne E, Pellas T. In vivo assessment of macromolecular content in articular cartilage of the goat knee. Magn Reson Med 2003; 49(6): 1037–1046.
6. Tiderius CJ, Olsson LE, Leander P, Ekberg O, Dahlberg L. Delayed gadolinium-enhanced MRI of cartilage (dGEMRIC) in early knee osteoarthritis. Magn Reson Med 2003; 49(3): 488–492.
7. Koenig SH, Baglin C, Brown RD, 3rd, Brewer CF. Magnetic field dependence of solvent proton relaxation induced by Gd^{3+} and Mn^{2+} complexes. Magn Reson Med 1984; 1(4): 496–501.
8. Stanisz GJ, Henkelman RM. Gd-DTPA relaxivity depends on macromolecular content. Magn Reson Med 2000; 44(5): 665–667.
9. Pintaske J, Martirosian P, Graf H, Erb G, Lodemann KP, Claussen CD, Schick F. Relaxivity of gadopentetate dimeglumine (Magnevist), gadobutrol (Gadovist), and gadobenate dimeglumine (MultiHance) in human blood plasma at 0.2, 1.5, and 3 Tesla. Invest Radiol 2006; 41(3): 213–221.
10. Giesel FL, von Tengg-Kobligk H, Wilkinson ID, Siegler P, von der Lieth CW, Frank M, Lodemann KP, Essig M. Influence of human serum albumin on longitudinal and transverse relaxation rates (r_1 and r_2) of magnetic resonance contrast agents. Invest Radiol 2006; 41(3): 222–228.
11. Bradley DA, Moger CJ, Winlove CP. Zn deposition at the bone-cartilage interface in equine articular cartilage. Nucl Instrum Methods Phys Res, Sect A 2007; 580(1): 473–476.
12. Pasqualicchio M, Gasperini R, Velo GP, Davies ME. Effects of copper and zinc on proteoglycan metabolism in articular cartilage. Mediators Inflamm 1996; 5(2): 95–99.
13. Becker JS. Inorganic Mass Spectrometry: Principles and Applications. John Wiley and Sons: Chichester, UK, 2007.
14. Becker JS, Matusch A, Becker JSu, Wu B, Palm C, Becker A, Salber D. Mass spectrometric imaging (MSI) of metals using advanced BrainMet techniques for biomedical research. Int J Mass Spectrom 2011; 307(1–3): 3–15.
15. Becker JS, Zoriy M, Matusch A, Wu B, Salber D, Palm C, Becker JSu. Bioimaging of metals by laser ablation inductvely coupled plasma mass spectromety (LA-ICP-MS). Mass Spectrom Rev 2010; 29(1):156–175.
16. Kamaly N, Pugh JA, Kalber TL, Bunch J, Miller AD, McLeod CW, Bell JD. Imaging of gadolinium spatial distribution in tumor tissue by laser ablation inductively coupled plasma mass spectrometry. Mol Imag Biol 2010; 12(4): 361–366.
17. Hsieh YK, Jiang PS, Yang BS, Sun TY, Peng HH, Wang CF. Using laser ablation/inductively coupled plasma mass spectrometry to bioimage multiple elements in mouse tumors after hyperthermia. Anal Bioanal Chem 2011; 401(3): 909–915.
18. Pugh JAT, Cox AG, McLeod CW, Bunch J, Whitby B, Gordon B, Kalber T, White E. A novel calibration strategy for analysis and imaging of biological thin sections by laser ablation inductively coupled plasma mass spectrometry. J Anal Atom Spectrom 2011; 26(8): 1667–1673.

19. Maroudas A. Physicochemical properties of cartilage in the light of ion exchange theory. Biophys J 1968; 8(5): 575–595.
20. Maroudas A, Bullough P, Swanson SA, Freeman MA. The permeability of articular cartilage. J Bone Joint Surg Br 1968; 50(1): 166–177.
21. Bullough PG, Yawitz PS, Tafra L, Boskey AL. Topographical variations in the morphology and biochemistry of adult canine tibial plateau articular cartilage. J Orthoped Res 1985; 3(1): 1–16.
22. Goodwin DW, Zhu H, Dunn JF. In vitro MR imaging of hyaline cartilage: correlation with scanning electron microscopy. AJR Am J Roentgenol 2000; 174(2): 405–409.
23. Langsjo TK, Hyttinen M, Pelttari A, Kiraly K, Arokoski J, Helminen HJ. Electron microscopic stereological study of collagen fibrils in bovine articular cartilage: volume and surface densities are best obtained indirectly (from length densities and diameters) using isotropic uniform random sampling. J Anat 1999; 195(Pt 2): 281–293.
24. Wiener E, Settles M, Weirich G, Schmidt C, Diederichs G. The Influence of Collagen Network Integrity on the Accumulation of Gadolinium-Based MR Contrast Agents in Articular Cartilage. Fortschritte auf dem Gebiet der Röntgenstrahlen und der bildgebenden Verfahren 2011.
25. Wiener E, Settles M, Diederichs G. T(2) relaxation time of hyaline cartilage in presence of different gadolinium-based contrast agents. Contrast Media Mol Imag 2010; 5(2): 99–104.
26. Wiener E, Woertler K, Weirich G, Rummeny EJ, Settles M. Contrast enhanced cartilage imaging: comparison of ionic and non-ionic contrast agents. Eur J Radiol 2007; 63(1): 110–119.
27. Xia Y, Zheng S, Bidthanapally A. Depth-dependent profiles of glycosaminoglycans in articular cartilage by microMRI and histochemistry. J Magn Reson Imag 2008; 28(1): 151–157.
28. Rizzo R, Grandolfo M, Godeas C, Jones KW, Vittur F. Calcium, sulfur, and zinc distribution in normal and arthritic articular equine cartilage: a synchrotron radiation-induced X-ray emission (SRIXE) study. J Exp Zool 1995; 273(1): 82–86.
29. Reinert T, Reibetanz U, Vogt J, Butz T, Werner A, Grunder W. Spatially resolved elemental distributions in articular cartilage. Nucl Instrum Meth Phys Res B 2001; 181: 516–521.
30. Alini M, Matsui Y, Dodge GR, Poole AR. The extracellular matrix of cartilage in the growth plate before and during calcification: changes in composition and degradation of type II collagen. Calcif Tissue Int 1992; 50(4): 327–335.
31. Becker JS, Jakubowski N. The synergy of elemental and biomolecular mass spectrometry: new analytical strategies in life sciences. Chem Soc Rev 2009; 38: 1969–1983.
32. Tibi M, Heumann K. Isotope dilution mass spectrometry as a calibration method for the analysis of trace elements in powder samples by LA-ICP-MS. J Anal Atom Spectrom 2003; 18(9): 1076–1081.
33. Boulyga SF, Desideri D, Meli MA, Testa C, Becker JS. Plutonium and americium determination in mosses by laser ablation ICP-MS combined with isotope dilution technique. Int J Mass Spectrom 2003; 226(3): 329–339.
34. Pickhardt C, Izmer AV, Zoriy MV, Schaumloffel D, Becker JS. On-line isotope dilution in laser ablation inductively coupled plasma mass spectrometry using a microflow nebulizer inserted in the laser ablation chamber. Int J Mass Spectrom 2006; 248(3):136–141.
35. Sela H, Karpas Z, Zoriy M, Pickhardt C, Becker JS. Biomonitoring of hair samples by laser ablation inductively coupled plasma mass spectrometry (LA-ICP-MS). Int J Mass Spectrom 2007; 261(2–3): 199–207.
36. Vogl J. Characterisation of reference materials by isotope dilution mass spectrometry. J Anal Atom Spectrom 2007; 22(5): 475–492.
37. Osterholt T, Salber D, Matusch A, Becker JS, Palm C. IMAGENA: image generation and analysis – an interactive software tool handling LA-ICP-MS data. Int J Mass Spectrom 2011; 307: 232–239.